

HILBERT CURVES IN TWO DIMENSIONS

CURVAS DE HILBERT EN DOS DIMENSIONES

E. ESTEVEZ-RAMS^{a†}, D. ESTEVEZ-MOYA^b, Y. MARTÍNEZ-CAMEJO^c, D. GÓMEZ-GÓMEZ^b AND BEATRIZ ARAGÓN-FERNÁNDEZ^d

a) Facultad de Física-IMRE, Universidad de La Habana, Cuba; estevez@imre.uh.cu[†]

b) Facultad de Matemática, University of Havana, San Lazaro y L. CP 10400, La Habana, Cuba

c) Instituto de Física, Universidade Federal de Uberlândia, 38408-100, Uberlândia-MG, Brasil

d) Universidad de Ciencias Informáticas, Carretera a San Antonio, La Habana, Cuba

[†] corresponding author

Recibido 4/2/2017; Aceptado 4/5/2017

The complete set of Hilbert curves in two dimensions is presented, comprising up to forty curves: 12 homogeneous and 28 inhomogeneous. The analytical expressions for all the homogeneous curves are derived, which are easily extendable to all forty curves. A tag system, that allows the construction of all curves, is also described.

El conjunto completo de curvas de Hilbert en dos dimensiones es presentado, comprendiendo cuarenta curvas: 12 homogéneas y 28 inhomogéneas. Las expresiones analíticas para todas las curvas inhomogéneas son deducidas, lo cual es fácilmente extensible a todas las curvas. Un sistema de tortuga, que permite la construcción de todas las curvas también es descrito.

PACS: Other topics in mathematical methods in physics, 02.90.+p; Computational techniques, simulations, 02.70.-c; Linear algebra, 02.10.Ud

I. INTRODUCTION

There is an important number of applications that involves or benefits from mapping points from a multidimensional space into a single dimension and viceversa. Locality preservation measures how points close together in the multidimensional space remain close when mapped to the one dimensional space. In data base applications, for example, it is often needed to map elements from a multidimensional attribute space onto a linear range of block addresses on the storage media. In such case, access speed could improve if points close together in the multi-dimensional attribute space are also close together in the one-dimensional space [1, 2], a property often related to clustering [3]. A similar need arises in image representation and storage, when a single numeric index is used to address each point in a multidimensional image space. Here, close regions in the multidimensional image space should correspond to consecutive values in the numerical index in such a way, that partial storage and retrieval could be optimized, as well as compression over the one dimensional sequence [4–6]. Another application is the visualization of massive one dimensional data as a two dimensional image that allows a global view of the data while the local features are not lost [7–9]. Other applications include bandwidth reduction [10], sub-optimal solution of the traveling salesman problem [11, 12].

Space filling curves allow a surjective mapping between the one dimensional space and the d -dimensional one: $\mathbb{R} \rightarrow \mathbb{R}^d$. In the two-dimensional case, the most studied space filling curve has been the Hilbert curve [13]. Iterative curve-generating algorithms are already well established, and allow to construct an onto, but not one-to-one, mapping between the unit segment $I = \{t | 0 \leq t \leq 1\}$ and the unit square $Q = \{(x, y) | 0 \leq x \leq 1, 0 \leq y \leq 1\}$ [14]. This mapping, as any other space filling curve mapping, is not a bijective one.

Nevertheless, its n^{th} -order iteration, or approximation, may indeed be seen as a bijective mapping between subsegments of I and subsquares of Q to a 4^n -resolution [15]. This, together with the good locality preservation through all the iterations, is what has opened a wealth of applications of the Hilbert curve in computer sciences [1, 2]; image processing [5, 16]; data visualization [8, 9]; antenna design [17, 18]; computer aided design [19]; pattern recognition [20]; passive radio frequency tag [21]; among others. Effective algorithms for the generation of Hilbert curves have been reported [22, 23].

Hilbert curves are based on the iterative application of affine transformations to a starting mapping [14]. In the starting mapping the unit interval is partitioned into four disjoint, equal length, subintervals, and put into correspondence with a four disjoint, equal area, subsquares partition of the unit square. At each step, each subinterval and corresponding subsquare, are considered as an original interval and square, respectively, and the affine transformation is then applied over them. The affine transformation must be so, that continuity is preserved, and also that two adjacent subintervals are mapped into two adjacent subsquares. The curve is uniquely defined (up to a rotation or reflection) by fixing the mapping of the initial and final subintervals.

After Hilbert original curve Moore [24] introduced a new curve that now bears his name. Liu [25] described four new curves, introducing a new approach for constructing other mappings. The affine transformations involved to obtain a n -order curve, involves only one iteration over the $(n - 1)$ -order Hilbert curve.

Pérez-Davidenko et al. [26] have further developed the idea by introducing the concept of homogeneous Hilbert curves (HHC) in two dimensions. HHC can be proper or improper. Homogeneity implies that only one set of rules is applied to the n^{th} -order Hilbert curve in order to

generate the $(n + 1)$ -order curve. The development is based on the idea that n -order space filling curves can be also built from $(n - 1)$ -order Liu curves, if the latter shows the correct quadrant connectivity. It was found that only the fourth Liu curve can be used for such purposes, and six additional curves can be added to complete twelve HHC in two dimensions [26].

If the homogeneity condition is dropped and it is allowed to build $n + 1$ -order curves by mixing Hilbert curves of different type at different quadrants, the set of Hilbert type curves can be further extended. Such curves will be named inhomogeneous and they expand the number of Hilbert curves in two dimensions up to forty.

The importance of finding new space filling curves is due to the fact that some of the above cited applications can improve their performance if a broader set, from where candidate solutions can be drawn, is available.

Analytical expressions for space filling curves was pioneered by Sagan [14]. The availability of closed expressions has several advantages, both practical and theoretical. It can be used as a starting point for generating algorithms, and it can be used to prove theorems involving the curves itself.

Séebold has showed that the original Hilbert curve could be seen as the realization of certain tag system, consisting in the application of a morphism to an infinite word [27]. The tag-system offers a simple and intuitive procedure to build the space filling curve of any order.

The aim of this contribution is to present, in a single paper, several results involving two dimensional Hilbert curves. The analytical expressions for all homogeneous curves are deduced and reported, this includes the proper and improper curves. We report how to extend the number of curves to include the inhomogeneous ones. A construction algorithm for all reported curves based on a tag system is also reported.

II. HILBERT CURVES CONSTRUCTION ALGORITHM

For the purpose of this paper, a 2D space filling curve is a surjective mapping of the unit interval I onto the unit square Q , $I \rightarrow Q$.

Remark II.1 An ordered tern (x, y) of rationals is called a point. A one-to-one mapping, whose domain is a finite ordered set $\{I\}$ of R rationals ($r \in \{I\}, 0 \leq r < 1$) and whose image is a set $\{Q\}$ of R points ($\zeta = (x, y) \in \{Q\}, 0 \leq x < 1, 0 \leq y < 1$), is called a curve mapping. If a point $\zeta \in \{Q\}$ is the image of a rational $r \in \{I\}$ under the mapping $f^{(k)}$ ($r \xrightarrow{f^{(k)}} \zeta$), then ζ is denoted by $f^{(k)}(r)$. In particular, if r_0 is the minimum (first) value in the ordered set $\{I\}$ ($r_0 < r \forall r \in \{I\}; r \neq r_0$) then $f^{(k)}(r_0)$ is called the entry point, and if r_{R-1} is the maximum (last) value in the ordered set $\{I\}$ ($r_{R-1} > r \forall r \in \{I\}; r \neq r_{R-1}$) then $f^{(k)}(r_{R-1})$ is called the exit point. In what follows, the set $\{I\}$ will consist of $R = 4^k$ rational values $n/4^k$, where $0 \leq n < 4^k - 1$, the entry point and exit points will be $f^{(k)}(0)$ and $f^{(k)}(1 - 1/4^k)$, respectively. Such set will be denoted by $I^{(k)}$. The corresponding set of 4^k points will be denoted by $Q^{(k)}$. The

mapping $f^{(k)}$ is called the k -order curve mapping. When $k \rightarrow \infty$ the superscript k will be dropped.

Remark II.2 We will say that a rational number $r \in [0, 1)$ has a quaternary representation (quaternary decomposition) denoted by $r = 0.q_1q_2q_3 \dots q_k$ ($0 \leq q_i < 4$) if

$$r = \frac{q_1}{4} + \frac{q_2}{4^2} + \frac{q_3}{4^3} + \dots + \frac{q_k}{4^k} \quad (0 \leq q_i < 4). \quad (1)$$

A rational number has a quaternary decomposition of order k if $q_i = 0 \quad \forall i > k$.

Remark II.3 For the purpose of this paper it will be called a R -partition of the unit interval I an ordered sequence of R non-overlapping segments I_i of equal length ($= 1/R$) such that $\bigcup_{i=1}^R I_i = I$. A quaternary partition of order k of the unit interval is a 4^k -partition of the unit interval. A recursive partition of an interval I is a partition of the unit interval such that, in each recursive step, each subsegment of the previous step is taken as a new interval to be partitioned. The partition segments are numbered from left to right. If the set $I^{(k)}$ is built by rational numbers r with quaternary decomposition of at most order k , then to each $r = 0.q_1q_2q_3 \dots q_k \in I^{(k)}$ will correspond the segment $\sum_{i=1}^k q_i 4^{k-i}$ in the recursive quaternary partition of order k of the unit interval which will be denoted by $I_{0.q_1q_2q_3 \dots q_k}$.

Remark II.4 For the purpose of this paper it will be called a R -partition of the unit square Q a set of R non-overlapping subsquares Q_j of equal area, such that $\bigcup_{j=1}^R Q_j = Q$. A quaternary partition of order k of the unit square is a 4^k -partition of the unit square. A recursive partition of the unit square Q is a partition such that, in each recursive step, each subsquare of the previous step is taken as a new square to be partitioned. In a quaternary recursive partition of a square Q_i each subsquare will be labeled in clockwise manner starting from the lower left (Figure 1). If $0.q_1q_2q_3 \dots q_k$ is the quaternary decomposition of some rational number r , then $Q_{0.q_1q_2q_3 \dots q_k}$ is the subsquare determined by the following recursive procedure: (i) Choose the unit square, make $i = 1$; (ii) Make a quaternary partition of the chosen square and choose the q_i subsquare, make $i = i + 1$; (iii) if $i < k$ return to step (ii), stop otherwise, $Q_{0.q_1q_2q_3 \dots q_k}$ is the last chosen subsquare. To each subsquare in the 4^k -partition of the unit square, a representative point can be assigned belonging to the subsquare, thus effectively building a $Q^{(k)}$ set of points. In this way, $f^{(k)}(r)$ will also denote a mapping between the partition of order k of the unit interval and the partition of the same order of the unit square.

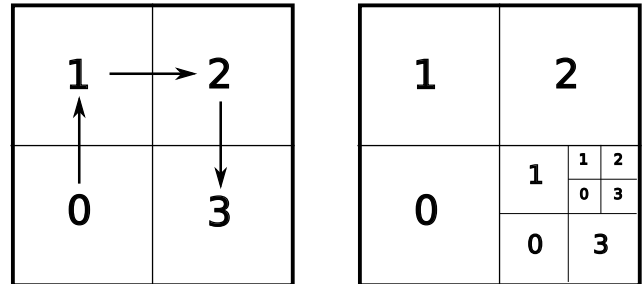


Figure 1. Recursive partition of the unit square.

The rationale behind Hilbert recursive construction of a space filling curves can be described by the following algorithm (Fig. 2):

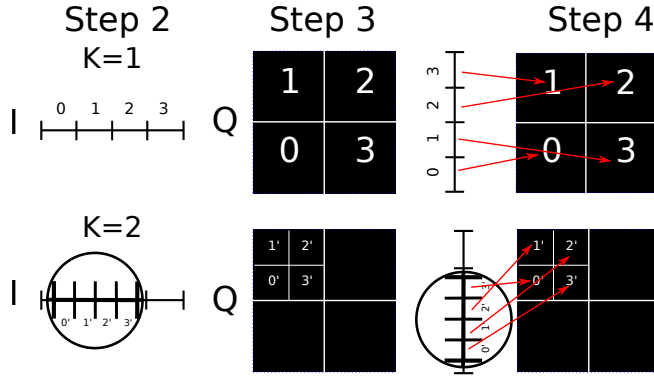


Figure 2. Hilbert construction.

1. $I_0 = \{r | 0 \leq r \leq 1\}$ and $Q_0 = \{(x, y) | 0 \leq x \leq 1, 0 \leq y \leq 1\}$, $k = 0$.

2. Perform a quaternary partition of each interval

$$I_{0.q_1 \dots q_k} \rightarrow I_{0.q_1 \dots q_k 0} \cup I_{0.q_1 \dots q_k 1} \cup I_{0.q_1 \dots q_k 2} \cup I_{0.q_1 \dots q_k 3}. \quad (2)$$

3. Perform a quaternary partition of each subsquare

$$Q_{0.m_1 \dots m_k} \rightarrow Q_{0.m_1 \dots m_k 0} \cup Q_{0.m_1 \dots m_k 1} \cup Q_{0.m_1 \dots m_k 2} \cup Q_{0.m_1 \dots m_k 3}. \quad (3)$$

4. Make the correspondence $I_{0.q_1 \dots q_k q_{k+1}} \rightarrow Q_{0.m_1 \dots m_k m_{k+1}}$ such that two consecutive segments in $I^{(k+1)}$ corresponds to two adjacent subsquares in $Q^{(k+1)}$ (adjacency condition), while preserving the continuity between the entry and exit point of each subsquare in the previous partition (continuity condition).

5. $k=k+1$

6. go to step 2.

The curve obtained at the k iteration is known as the Hilbert curve of order k , and will correspond to the partition of the unit interval and the unit square into 4^k subintervals and subsquares, respectively. The algorithm described above does not determine uniquely the curve mapping, in order to do so, boundary condition must be given. That is, for all k , fix the entry and exit point, i.e. the mapping of the initial and final segment to the corresponding subsquares in the quaternary partition of Q . Hilbert curves are usually referred to the infinite limit $k \rightarrow \infty$, where the mapping becomes surjective.

Hilbert original curve results from mapping at any order k , the entry point as the lower left subsquare ($I_{0.000 \dots 0} \rightarrow Q_{0.000 \dots 0}$); and the exit point to the lower right subsquare ($I_{0.333 \dots 3} \rightarrow Q_{0.333 \dots 3}$).

III. HOMOGENEOUS HILBERT CURVES

Definition III.1 An homogeneous Hilbert curve (HHC) of order k is a Hilbert curve of order k built recursively from one and only one Hilbert curve of order $k - 1$.

By assigning different initial and final mappings, five additional curves, besides the original Hilbert curve, can be constructed. These curves have been called by Davidenko et al. proper Hilbert curves [26]. The boundary conditions for the complete set of proper Hilbert curve can be seen in Table III and Figure 3.

Table 1. The boundary conditions for the set of Hilbert proper curves.

v	Curve	Boundary conditions
0	Hilbert	$I_{0.000 \dots 0} \rightarrow Q_{0.000 \dots 0}$ $I_{0.333 \dots 3} \rightarrow Q_{0.333 \dots 3}$
1	Moore	$I_{0.000 \dots 0} \rightarrow Q_{0.033 \dots 3}$ $I_{0.333 \dots 3} \rightarrow Q_{0.300 \dots 0}$
2	Liu 1	$I_{0.000 \dots 0} \rightarrow Q_{0.022 \dots 2}$ $I_{0.333 \dots 3} \rightarrow Q_{0.311 \dots 1}$
3	Liu 2	$I_{0.000 \dots 0} \rightarrow Q_{0.011 \dots 1}$ $I_{0.333 \dots 3} \rightarrow Q_{0.322 \dots 2}$
4	Liu 3	$I_{0.000 \dots 0} \rightarrow Q_{0.000 \dots 0}$ $I_{0.333 \dots 3} \rightarrow Q_{0.311 \dots 1}$
5	Liu 4	$I_{0.000 \dots 0} \rightarrow Q_{0.011 \dots 1}$ $I_{0.333 \dots 3} \rightarrow Q_{0.300 \dots 0}$

Remark III.2 The proper Hilbert curve of order k is given the symbol ${}_v H_k$, with $v = 0, 1, 2 \dots 5$, where ${}_0 H_k$ and ${}_1 H_k$ are Hilbert's original curve and the Moore's curve [24], respectively. For $v = 2, 3, 4, 5$ the symbols correspond to the additional proper curves introduced by Liu [25].

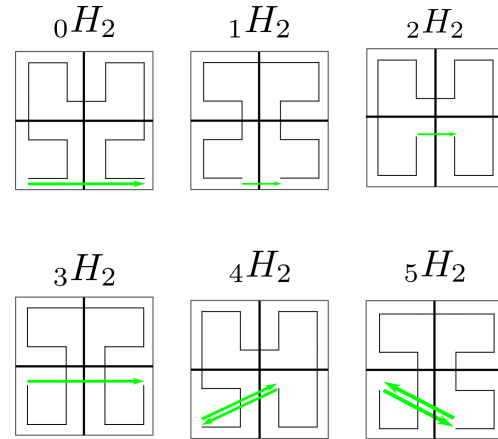


Figure 3. Boundary vectors (shown in green) of all six proper homogeneous Hilbert curves. ${}_4 H$ and ${}_5 H$ are not mirror symmetric, which results in two boundary vectors related by the reversion operation. Boundary vector for Hilbert curve ${}_2 H$ can not be used for building improper Hilbert curves as it is the only boundary vector that starts and ends at interior points of the Hilbert curve.

Consider an additional operation called reversion. Reversion swaps the entry and exit point of a curve mapping (Figure 4). If the reversion operation is introduced, six additional curves called improper in [26] can be constructed. The boundary conditions for the complete set of improper Hilbert curve of order $k > 2$ can be seen in Table III.

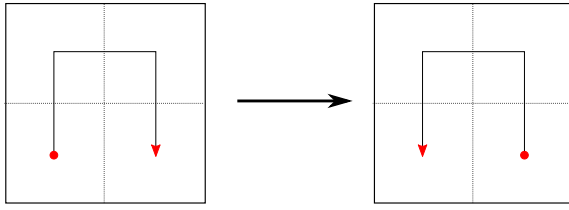


Figure 4. Reversion operation.

Table 2. The boundary conditions for the set of Hilbert improper curves with order larger than 3.

ν	Curve	Boundary conditions
6	I1	$I_{0.000...0} \rightarrow Q_{0.023...3}$ $I_{0.333...3} \rightarrow Q_{0.310...0}$
7	I2	$I_{0.000...0} \rightarrow Q_{0.023...3}$ $I_{0.333...3} \rightarrow Q_{0.332...2}$
8	I3	$I_{0.000...0} \rightarrow Q_{0.001...1}$ $I_{0.333...3} \rightarrow Q_{0.332...2}$
9	I4	$I_{0.000...0} \rightarrow Q_{0.032...2}$ $I_{0.333...3} \rightarrow Q_{0.301...1}$
10	I5	$I_{0.000...0} \rightarrow Q_{0.010...0}$ $I_{0.333...3} \rightarrow Q_{0.323...3}$
11	I6	$I_{0.000...0} \rightarrow Q_{0.010...0}$ $I_{0.333...3} \rightarrow Q_{0.301...1}$

Table 3. Geometric properties of HHC.

Curve	Symm.	Entry-Exit points	Closed
${}_0H$ (Hilbert)	m	corner-corner	
${}_1H$ (Moore)	m	edge-edge shared	X
${}_2H$ (Liu1)	m	interior-interior	X
${}_3H$ (Liu2)	m	edge-edge opposed	
${}_4H$ (Liu3)	1	corner-interior	
${}_5H$ (Liu4)	1	edge-edge adjacent	
${}_6H$ (I1)	m	interior-interior	X
${}_7H$ (I2)	1	interior-edge	
${}_8H$ (I3)	m	edge-edge opposed	
${}_9H$ (I4)	m	interior-interior	X
${}_{10}H$ (I5)	m	edge-edge opposed	
${}_{11}H$ (I6)	1	edge-interior	

Proper curves of order k are constructed from a specific mapping, different for each curve type, over the ${}_0H_{k-1}$ curve. Improper curves, on the other hand, are constructed from a specific mapping, different for each curve type, over the ${}_5H_{k-1}$ (Liu 4) curve.

Figure 5 shows the twelve possible HHC of order 4.

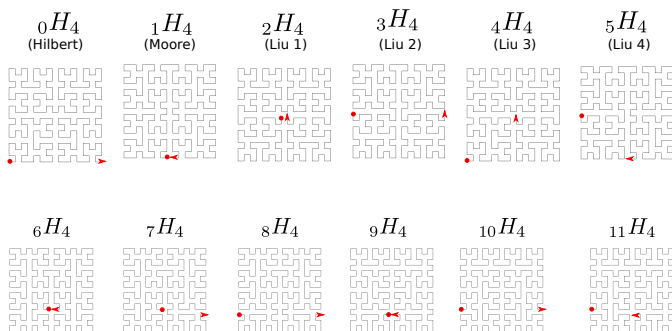


Figure 5. The homogeneous Hilbert curves of order 4. The circle signals the entry point, and the arrow the exit point.

From a geometric point of view HHC can be classified by their symmetry: some curves possess a vertical symmetry line at the middle of the unit square (m symmetry); they can also be classified according to the nature of the entry and exit points, which can lie at a corner, edge or interior subsquare; finally HHC can be closed if the entry and exit point lies at adjacent subsquares (Table III).

IV. ARITHMETIC REPRESENTATION OF HHC

The HHC can also be described as generated iteratively by the application of certain sets of affine transformations ${}_v p_i$ to points $\zeta = (x, y)$ belonging to the unit square. The affine transformation operator has the general form

$$p \begin{pmatrix} x \\ y \end{pmatrix} = \frac{1}{2} \mathbf{U} \cdot \begin{pmatrix} x \\ y \end{pmatrix} + \frac{1}{2} \mathbf{t} = [U, t]_{\frac{1}{2}} \begin{pmatrix} x \\ y \end{pmatrix}, \quad (4)$$

where \mathbf{U} is a rotation, given by a 2×2 orthogonal matrix, and \mathbf{t} is a two dimensional translation vector. Each ${}_v H_k$ is constructed by using a set of four ${}_v P = \{{}_v p_i\}$ ($i = 0, 1, 2, 3$) transformations, one for each quadrant, that act (\otimes) over the coordinates of the $k - 1$ -order curve. For the proper curves, the operation can be formally represented as

$${}_v H_n = {}_v P \otimes {}_0 H_{n-1}, \quad (5)$$

while for the improper curves

$${}_v H_n = {}_v P \otimes {}_5 H_{n-1}. \quad (6)$$

Table 4 gives the sets of affine transformations.

Table 4. Affine transformations $p = [U, t]_{\frac{1}{2}}$ for the HHC. (The $\frac{1}{2}$ subscript is dropped for succinctness. The over-bar means reversion operation, see [26] for details).

Curve	q_0	q_1	q_2	q_3
${}_0H$ (Hilbert)	$[U_R, t_0]$	$[U_I, t_1]$	$[U_I, t_3]$	$[-U_R, t_4]$
${}_1H$ (Moore)	$[U_V, t_2]$	$[U_V, t_3]$	$[-U_V, t_5]$	$[-U_V, t_3]$
${}_2H$ (Liu 1)	$[-U_I, t_3]$	$[U_I, t_1]$	$[U_I, t_3]$	$[-U_I, t_4]$
${}_3H$ (Liu 2)	$[U_H, t_1]$	$[U_V, t_3]$	$[-U_V, t_5]$	$[U_H, t_3]$
${}_4H$ (Liu 3)	$[U_R, t_0]$	$[U_I, t_1]$	$[U_I, t_3]$	$[-U_I, t_4]$
${}_5H$ (Liu 4)	$[U_H, t_1]$	$[U_V, t_3]$	$[-U_V, t_5]$	$[-U_V, t_3]$
${}_6H$ (I1)	$[-U_I, t_3]$	$[-U_H, t_3]$	$[U_I, t_3]$	$[U_H, t_3]$
${}_7H$ (I2)	$[-U_I, t_3]$	$[-U_H, t_3]$	$[U_I, t_3]$	$[-U_R, t_4]$
${}_8H$ (I3)	$[-U_V, t_1]$	$[-U_H, t_3]$	$[U_I, t_3]$	$[-U_R, t_4]$
${}_9H$ (I4)	$[-U_R, t_3]$	$[U_V, t_3]$	$[U_R, t_3]$	$[-U_V, t_3]$
${}_{10}H$ (I5)	$[U_H, t_1]$	$[U_V, t_3]$	$[U_R, t_3]$	$[-U_I, t_4]$
${}_{11}H$ (I6)	$[U_H, t_1]$	$[U_V, t_3]$	$[U_R, t_3]$	$[-U_V, t_3]$

$$U_I = \begin{pmatrix} 1 & 0 \\ 0 & 1 \end{pmatrix} \quad U_R = \begin{pmatrix} 0 & 1 \\ 1 & 0 \end{pmatrix}$$

$$U_V = \begin{pmatrix} 0 & -1 \\ 1 & 0 \end{pmatrix} \quad U_H = \begin{pmatrix} 1 & 0 \\ 0 & -1 \end{pmatrix}$$

$$t_0 = \begin{pmatrix} 0 \\ 0 \end{pmatrix} \quad t_1 = \begin{pmatrix} 0 \\ 1 \end{pmatrix} \quad t_2 = \begin{pmatrix} 1 \\ 0 \end{pmatrix}$$

$$t_3 = \begin{pmatrix} 1 \\ 1 \end{pmatrix} \quad t_4 = \begin{pmatrix} 2 \\ 1 \end{pmatrix} \quad t_5 = \begin{pmatrix} 1 \\ 2 \end{pmatrix}$$

The rotation matrices of the affine transformations form a group. The multiplication table is shown in Table 5.

The group is isomorphic with the planar point group 4mm [28] with generators $\{U_R, U_H\}$. The group structure exhibits three subgroups of order 4: $\{U_I, -U_I, U_R, -U_R\}$ and $\{U_I, -U_I, U_H, -U_H\}$ isomorphic to 2mm, $\{U_I, -U_I, U_V, -U_V\}$ isomorphic to the planar point group 4; five cyclic subgroups of order two: $\{U_I, U_R\}$, $\{U_I, -U_R\}$, $\{U_I, -U_I\}$, $\{U_I, U_H\}$, $\{U_I, -U_H\}$.

Table 5. The multiplication table for the rotation parts of the affine transformations. The rotation operations are defined in Table 4.

	U_I	U_R	$-U_I$	$-U_R$	U_V	U_H	$-U_V$	$-U_H$
U_I	U_I	U_R	$-U_I$	$-U_R$	U_V	U_H	$-U_V$	$-U_H$
U_R	U_R	U_I	$-U_R$	$-U_I$	U_H	U_V	$-U_H$	$-U_V$
$-U_I$	$-U_I$	$-U_R$	U_I	U_R	$-U_V$	$-U_H$	U_V	U_H
$-U_R$	$-U_R$	$-U_I$	U_R	U_I	$-U_H$	$-U_V$	U_H	U_V
U_V	U_V	$-U_H$	$-U_V$	U_H	$-U_I$	U_R	U_I	$-U_R$
U_H	U_H	$-U_V$	$-U_H$	U_V	$-U_R$	U_I	U_R	$-U_I$
$-U_V$	$-U_V$	U_H	U_V	$-U_H$	U_I	$-U_R$	$-U_I$	U_R
$-U_H$	$-U_H$	U_V	U_H	$-U_V$	U_R	$-U_I$	$-U_R$	U_I

We now generalize the procedure for an analytic representation of the original Hilbert curve ${}_0H$ given by Sagan [14] to include all HHC.

Theorem IV.1 Consider a rational number $r \in I^{(k)}$ with quaternary representation of order k given by equation (1). The curve mapping $f_v^{(k)}$ of the proper ${}_vH_k$ Hilbert curve ($v \leq 5$) will be given by

$$f_v^{(k)}(r) = \left(\frac{1}{2^k}\right) {}_vU_{q_1} {}_0U_{q_2} \dots {}_0U_{q_k} \Omega + \sum_{j=2}^k \left(\frac{1}{2^j}\right) {}_vU_{q_1} {}_0U_{q_2} \dots {}_0U_{q_{k-1}} {}_0t_{q_j} + \frac{1}{2} {}_vt_{q_1}, \quad (7)$$

where Ω is the set $Q^{(0)}$ with a representative point for the unit square.

Proof. According to equation (5),

$$\begin{aligned} {}_vH_n &= {}_vP \otimes {}_0H_{n-1} = {}_vP \otimes {}_0P \otimes {}_0H_{n-2} = \\ &= {}_vP \otimes {}_0P \otimes {}_0P \otimes {}_0H_{n-3} = \\ &\dots \\ &= {}_vP \otimes \overbrace{{}_0P \otimes {}_0P \otimes \dots \otimes {}_0P}^k \otimes {}_0H_0 \end{aligned}$$

each ${}_vP$ in the above expression is a set of four affine transformations that defines the curve mapping. If we consider I_r with $r = 0.q_1q_2\dots q_k$ then expression (8) determines by construction the curve mapping:

$$f_v^{(k)}(r) = {}_vp_{q_1} {}_0p_{q_2} {}_0p_{q_3} \dots {}_0p_{q_k} \Omega \quad (9)$$

where Ω , without loss of generality, will be taken as $\Omega =$

$\{(1/2, 1/2)\}$. From equation (4)

$$\begin{aligned} f_v^{(k)}(r) &= {}_vp_{q_1} {}_0p_{q_2} {}_0p_{q_3} \dots {}_0p_{q_{k-1}} \left[\frac{1}{2} {}_0U_{q_k} \Omega + \frac{1}{2} {}_0t_{q_k} \right] = \\ &= {}_vp_{q_1} {}_0p_{q_2} {}_0p_{q_3} \dots {}_0p_{q_{k-2}} \left[\frac{1}{2} {}_0U_{q_{k-1}} \left[\frac{1}{2} {}_0U_{q_k} \Omega + \frac{1}{2} {}_0t_{q_k} \right] + \frac{1}{2} {}_0t_{q_{k-1}} \right] = \\ &= {}_vp_{q_1} {}_0p_{q_2} {}_0p_{q_3} \dots {}_0p_{q_{k-2}} \left[\frac{1}{2^2} {}_0U_{q_{k-1}} {}_0U_{q_k} \Omega + \frac{1}{2^2} {}_0U_{q_{k-1}} {}_0t_{q_k} + \frac{1}{2} {}_0t_{q_{k-1}} \right] = \\ &= \dots \end{aligned}$$

and expanding for all operators we arrive at equation (7). \square

Equation (7) gives the arithmetic representation of a Hilbert curve of order k : ${}_vH_k$.

Corollary IV.2 In the limit $k \rightarrow \infty$,

$$f_v(r) = \sum_{j=2}^{\infty} \left(\frac{1}{2^j}\right) {}_vU_{q_1} {}_0U_{q_2} \dots {}_0U_{q_{k-1}} {}_0t_{q_j} + \frac{1}{2} {}_vt_{q_1}. \quad (10)$$

Proof. It follows directly from equation (7), taking $k \rightarrow \infty$ makes the first term tend to zero. \square

From the multiplication table (Table 5), $-U_I = -U_R \cdot U_R$, where U_I is the identity matrix, which simplifies equation (7) to

$$\begin{aligned} f_v^{(k)}(r) &= \left(\frac{1}{2^k}\right) (-1)^{\#_3(2,k)} {}_vU_{q_1} \times \Omega + \sum_{j=2}^k \left(\frac{1}{2^j}\right) (-1)^{\#_3(2,j-1)} {}_vU_{q_1} \times \\ &\times U_R^{\#_{03}(2,j-1)} {}_0t_{q_j} + \frac{1}{2} {}_vt_{q_1}, \end{aligned}$$

use have been made of the fact that $U_R \Omega = \Omega$. $\#_3(s, p)$ is the number of 3s, from q_s to q_p , in the quaternary expansion of r ; correspondingly, $\#_{03}(s, p)$ is the number of 0s and 3s, from q_s to q_p , in the quaternary expansion of r :

$$\begin{aligned} \#_3(s, p) &= \frac{1}{6} \sum_{m=s}^p q_m(q_m - 2)(q_m - 1) \\ \#_{03}(s, p) &= p + \frac{1}{2} \sum_{m=s}^p q_m(q_m - 3) \end{aligned}$$

If $\#_{03}(s, p)$ is even, then $U_R^{\#_{03}(s,p)} = U_I$ the identity operator, otherwise, $U_R^{\#_{03}(s,p)} = U_R$.

Theorem IV.3 Consider a rational number $r \in I^{(k)}$ with quaternary representation of order k given by equation (1). If $f_v^{(k)}(r)$ is the image point of r for the ${}_vH_k$ proper curve, and $f_{v'}^{(k)}(r)$ is the image point of r for the ${}_{v'}H_k$ proper curve, then

$$f_v^{(k)}(r) = {}_vp_{q_1} {}_{v'}p_{q_1}^{-1} f_{v'}^{(k)}(r) \quad (11)$$

Proof. According to equation (9),

$$\begin{aligned} f_0^{(k)}(r) &= {}_0p_{q_1} {}_0p_{q_2} {}_0p_{q_3} \dots {}_0p_{q_k} \Omega \\ \text{from where} \\ {}_0p_{q_1}^{-1} f_0^{(k)}(r) &= {}_0p_{q_2} {}_0p_{q_3} \dots {}_0p_{q_k} \Omega, \end{aligned} \quad (12)$$

comparing equation (12) with equation (9), results in

$$f_v^{(k)}(r) = {}_vp_{q_1} {}_0p_{q_1}^{-1} f_0^{(k)}(r).$$

From this last equation, for two Hilbert curves ${}_v H_k$ and ${}_{v'} H_k$

$$\begin{aligned} f_0^{(k)}(r) &= {}_0 p_{q_1} {}_v p_{q_1}^{-1} f_v^{(k)}(r) \\ f_0^{(k)}(r) &= {}_0 p_{q_1} {}_{v'} p_{q_1}^{-1} f_{v'}^{(k)}(r), \end{aligned}$$

equation (11) follows immediately. \square

Expression (11) maps one-to-one a point in the proper Hilbert curve ${}_v H_k$ with its corresponding (in the sense of belonging to the same value $r \in I^{(k)}$) point in another proper Hilbert curve ${}_{v'} H_k$.

From equation (11), two points lying in the same quadrant preserve their distance when changing from one Hilbert curve to another. Indeed, if two points r and r_1 are mapped to the same quadrant, then in their quaternary decomposition, the share the same q_1 value, and

$$\begin{aligned} |f_v^{(k)}(r) - f_v^{(k)}(r_1)| &= \\ |{}_v p_{q_1} {}_{v'} p_{q_1}^{-1} f_{v'}^{(k)}(r) - {}_v p_{q_1} {}_{v'} p_{q_1}^{-1} f_{v'}^{(k)}(r_1)| &= \\ = |{}_v U_{q_1} {}_{v'} U_{q_1}^{-1} [f_{v'}^{(k)}(r) - f_{v'}^{(k)}(r_1)]| &= \\ = |{}_v U_{q_1}| |{}_v U_{q_1}^{-1}| |f_{v'}^{(k)}(r) - f_{v'}^{(k)}(r_1)| &= \\ = |f_{v'}^{(k)}(r) - f_{v'}^{(k)}(r_1)| \end{aligned}$$

where in the last step, use have been of the orthogonality of the ${}_v U$ in the affine transformations.

IV.1. Improper HHC

Theorem IV.4 Consider $r \in [0, 1]$ with k order quaternary decomposition, then given the one-to-one mapping $r \rightarrow r'$ given by Table 6, let the quaternary expansion of r' be given by equation (1). The curve mapping $f_v^{(k)}(r)$ of the improper ${}_v H_k$ Hilbert curve ($v \geq 6$) will be given by

$$\begin{aligned} f_v^{(k)}(r) &= \left(\frac{1}{2^k}\right) {}_v U_{q_1} {}_5 U_{q_2} {}_0 U_{q_3} \dots {}_0 U_{q_k} \Omega + \\ &+ \sum_{j=3}^k \left(\frac{1}{2^j}\right) {}_v U_{q_1} {}_5 U_{q_2} {}_0 U_{q_3} \dots {}_0 U_{q_{k-1}} {}_0 t_{q_j} + \\ &+ \frac{1}{4} {}_v U_{q_1} {}_5 t_{q_2} + \frac{1}{2} {}_v t_{q_1}. \end{aligned} \quad (13)$$

Table 6. Transformation of value r ($r \rightarrow r'$) for the improper ${}_v H_k$, before using equation (13).

$\lfloor 4r \rfloor$	0	1	2	3
${}_6 H$ (I1)	r	$3/4 - 1/4^k - r$	r	$7/4 - 1/4^k - r$
${}_7 H$ (I2)	r	$3/4 - 1/4^k - r$	r	r
${}_8 H$ (I3)	$1/4 - 1/4^k - r$	$3/4 - 1/4^k - r$	r	r
${}_9 H$ (I4)	$1/4 - 1/4^k - r$	r	$5/4 - 1/4^k - r$	r
${}_{10} H$ (I5)	r	r	$5/4 - 1/4^k - r$	$7/4 - 1/4^k - r$
${}_{11} H$ (I6)	r	r	$5/4 - 1/4^k - r$	r

Proof. For the improper curve mapping, following expression (6),

$$\begin{aligned} f_v^{(k)}(r) &= {}_v p_{q_1} {}_5 p_{q_2} {}_0 p_{q_3} \dots {}_0 p_{q_k} \Omega \\ &= {}_v p_{q_1} f_5^{(k-1)}(0.q_2 q_3 \dots q_k) \end{aligned} \quad (14)$$

expression (13) follows from (14) by the same reasoning used for the proper Hilbert curve mapping. In the case of improper curves, reversion operation must be taken care of. The integer part of $4r$ ($\lfloor 4r \rfloor$) determines to which quadrant in the quaternary partition of the unit square r will be mapped to. Table 4 shows which quadrant implies reversion and Table 6 follows directly. \square

Note that the quaternary expansion used in (13) is that of r' .

Corollary IV.5 In the limit $k \rightarrow \infty$ equation (13) reduces to

$$\begin{aligned} f_v(r) &= \\ \sum_{j=3}^{\infty} \left(\frac{1}{2^j}\right) {}_v U_{q_1} {}_5 U_{q_2} {}_0 U_{q_3} \dots {}_0 U_{q_{k-1}} {}_0 t_{q_j} + \\ \frac{1}{4} {}_v U_{q_1} {}_5 t_{q_2} + \frac{1}{2} {}_v t_{q_1}. \end{aligned} \quad (15)$$

Theorem IV.6 If $f_v^{(k)}(r)$ is the image point of r for the ${}_v H_k$ improper curve and, $f_{v'}^{(k)}(r)$ is the image point of r for the ${}_{v'} H_k$ improper curve, then

$$f_v^{(k)}(r) = {}_v p_{q_1} {}_{v'} p_{q_1}^{-1} f_{v'}^{(k)}(r) \quad (16)$$

Proof. Similar to the demonstration of corollary IV.3 \square

V. BUILDING HHC BASED ON A TAG SYSTEM

Consider the finite alphabet Σ , whose elements are called letters, and let Σ^* be the free monoid generated by Σ whose elements are called words (Σ^* is the set of all finite length words formed by the concatenation of letters drawn from Σ). The empty word ε is considered to be a member of Σ^* . The concatenation of two words p and s is written as ps . The length of a word p is denoted by $|p|$

Remark V.1 For the purposes of this article, a morphisms on Σ , is a map $\varphi : \Sigma^* \rightarrow \Sigma^*$, such that $\varphi(ps) = \varphi(p)\varphi(s)$ for all $p, s \in \Sigma^*$. A literal morphism is a morphism that preserves length, that is $|\varphi(p)| = |p|$. A non-erasing morphism is a morphism ϕ such that $\phi(a) \neq \varepsilon$ for all $a \in \Sigma$.

Remark V.2 In what follows, a tag system will be understood as a quintuple $T = (\Sigma, p, \phi, \varphi, \Sigma)$, where Σ is an alphabet; $p \in \Sigma^*$, $|p| > 0$; ϕ is a non-erasing morphism and φ a literal morphisms, both from Σ^* to Σ^* . If $\phi^n(p)$ ($n \in \mathbb{N}$) denotes the n -th application of the non-erasing morphism ϕ over the word p , then $\varphi(\phi^n(p))$ generates a word h of length $|h| \geq |p|$.

Let us consider the alphabet $\Sigma = \{u, d, l, r\}$, where u (d) stands for up (down), and l (r) stands for left (right). From a geometrical point of view, each letter from left to right in a word $p \in \Sigma$ can be seen as a pencil stroke of a unit length in the direction given by the letter. Then every Hilbert curve of any order can be described by a corresponding word in Σ^* (e.g. ${}_0 H_2$ in figure 3 will be described by the word $ruluurdrurddl$).

Define the morphism:

$$\begin{aligned} \delta_o(u) = r \quad \delta_o(r) = u \quad \delta_o(d) = l \quad \delta_o(l) = d \\ \delta_a(u) = l \quad \delta_a(r) = d \quad \delta_a(d) = r \quad \delta_a(l) = u, \end{aligned}$$

then the ${}_0H_{n+1}$ Hilbert curve can be constructed from the ${}_0H_n$ curve by the tag system given by ${}_0h_{n+1} = \delta_o({}_0h_n) u {}_0h_n r {}_0h_n d \delta_a({}_0h_n)$.

In a similar fashion the tag system for the remaining homogeneous Hilbert curves was given in [26] and repeated here for completeness. For the proper curves:

$$\begin{aligned} {}_1h_{n+1} &= \delta_g({}_0h_n) u \delta_g({}_0h_n) r \delta_x({}_0h_n) d \delta_x({}_0h_n) \\ {}_2h_{n+1} &= \delta_f({}_0h_n) u {}_0h_n r {}_0h_n d \delta_f({}_0h_n) \\ {}_3h_{n+1} &= \delta_m({}_0h_n) u \delta_g({}_0h_n) r \delta_x({}_0h_n) d \delta_m({}_0h_n) \\ {}_4h_{n+1} &= \delta_o({}_0h_n) u {}_0h_n r {}_0h_n d \delta_f({}_0h_n) \\ {}_5h_{n+1} &= \delta_m({}_0h_n) u \delta_g({}_0h_n) r \delta_x({}_0h_n) d \delta_x({}_0h_n). \end{aligned}$$

Considering \bar{p} as the reversion operation over the word p , given by reversing the order of the word and swapping left and right ($l \rightleftharpoons r$), as well as up and down ($u \rightleftharpoons d$) (e.g. $\text{ruluurdrurddldr} = \text{luruuldlulddrdl}$), the tag system for the improper curves will be:

$$\begin{aligned} {}_6h_{n+1} &= \delta_f({}_5h_n) u \overline{\delta_y({}_5h_n)} r {}_5h_n d \overline{\delta_a({}_5h_n)} \\ {}_7h_{n+1} &= \delta_f({}_5h_n) u \overline{\delta_y({}_5h_n)} r {}_5h_n d \delta_a({}_5h_n) \\ {}_8h_{n+1} &= \overline{\delta_x({}_5h_n)} u \overline{\delta_y({}_5h_n)} r {}_5h_n d \delta_a({}_5h_n) \\ {}_9h_{n+1} &= \delta_a({}_5h_n) u \delta_g({}_5h_n) r \overline{\delta_o({}_5h_n)} d \delta_x({}_5h_n) \\ {}_{10}h_{n+1} &= \delta_m({}_5h_n) u \delta_g({}_5h_n) r \overline{\delta_o({}_5h_n)} d \delta_f({}_5h_n) \\ {}_{11}h_{n+1} &= \delta_a({}_5h_n) u \delta_g({}_5h_n) r \overline{\delta_o({}_5h_n)} d \delta_x({}_5h_n). \end{aligned}$$

The morphism used above are defined as:

$$\begin{aligned} \delta_g(u) = l \quad \delta_g(r) = u \quad \delta_g(d) = r \quad \delta_g(l) = d \\ \delta_x(u) = r \quad \delta_x(r) = d \quad \delta_x(d) = l \quad \delta_x(l) = u \\ \delta_f(u) = d \quad \delta_f(r) = l \quad \delta_f(d) = u \quad \delta_f(l) = r \\ \delta_m(u) = d \quad \delta_m(r) = r \quad \delta_m(d) = u \quad \delta_m(l) = l \\ \delta_y(u) = u \quad \delta_y(r) = l \quad \delta_y(d) = d \quad \delta_y(l) = r \end{aligned}$$

VI. INHOMOGENEOUS HILBERT CURVES

If the homogeneity condition is dropped and it is allowed to build $k+1$ -order curves by mixing Hilbert curves of different type at different quadrants, the set of Hilbert type curves can be further extended. The following then takes relevance:

Definition VI.1 An inhomogeneous Hilbert curve (IHHC) of order k , is a Hilbert curve of order k built recursively from at least two different type Hilbert curve of order $k-1$.

The following theorem will be proved:

Theorem VI.2 There are forty different (up to a rotation, reflection or reversion) Hilbert curves in two dimensions: twelve homogeneous and twenty eight inhomogeneous.

Proof. A constructive geometric proof will be made based on boundary vectors similar to the one given in [26]. We already showed the twelve homogeneous Hilbert curve. These curves have exhausted all homogeneous possibilities as proved in [26]

Hilbert curves are uniquely determined by their boundary vectors which are preserved for any order [14,24]. All Hilbert curves can be explored by considering at each quadrant, the boundary vector. The set of all possible Hilbert curves in two dimensions can be exhausted, regardless of the curve order, by combining all possible boundary vectors at each quadrant in such a way that connected quadrants must have connected boundary vectors.

Except for Hilbert curve ${}_2H$ (both entry and exit point are interior, excluding the possibility of quadrant connectivity), all the other curves can serve as building blocks.

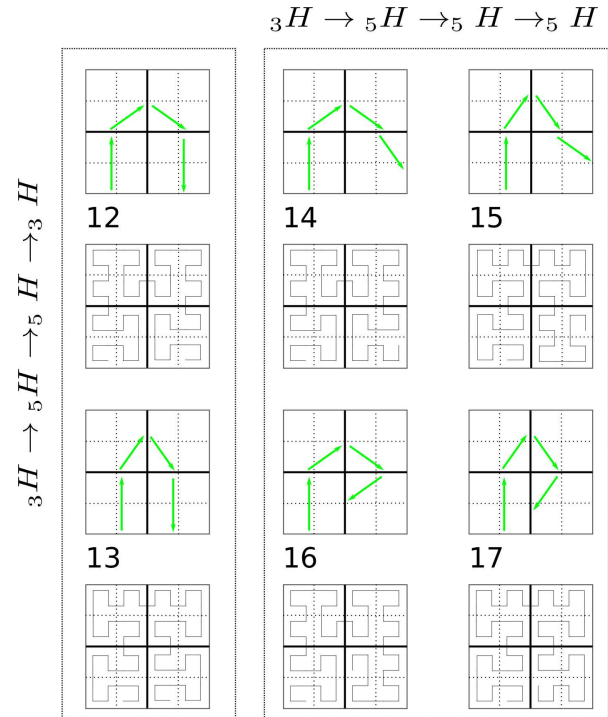


Figure 6. Inhomogeneous Hilbert curve built from the combination of ${}_3H$ and ${}_5H$ curves. Boundary vector diagrams and order 3 approximations.

For building the inhomogeneous Hilbert curve it must be first observed that, as already known, the boundary vector for ${}_0H_n$ and ${}_5H_n$ can be used at any quadrant. The boundary vector for the ${}_3H_n$ curve connects opposite edges (Figure 3) and, according to the connectivity diagram between quadrants shown in Figure 1a, it can only appear in the first and last quadrant. For the boundary vector of the ${}_4H_n$ curve, one end is an interior point and therefore, useless for quadrant connectivity. This constrains the use of such curve also to the first and last quadrants where connectivity are not required at one end. Finally, the boundary vector for the ${}_1H_n$ curve starts and ends at the same edge making it only useful at the first and last quadrants.

All possible combinations are then:

1. ${}_3H+{}_0H$: The boundary vectors of the ${}_3H$ and ${}_0H$ can only

connect quadrants: $0 \rightarrow 1$ or $2 \rightarrow 3$, as the boundary vector for the ${}_0H$ starts and ends at corners, while that of ${}_3H$ start and ends at the middle of edges.

2. ${}_3H + {}_5H$: The possible quadrants combinations of the boundary vectors will be: (a) ${}_3H \rightarrow {}_5H \rightarrow {}_5H \rightarrow {}_3H$. Another possibility is an ${}_3H$ in the first quadrant and three ${}_5H$ in the remaining quadrants: (b) ${}_3H \rightarrow {}_5H \rightarrow {}_5H \rightarrow {}_5H$. Taking into account rotation at quadrants 1 and 2, (a) and (b) results in a total of six new curves shown in Figure 6.

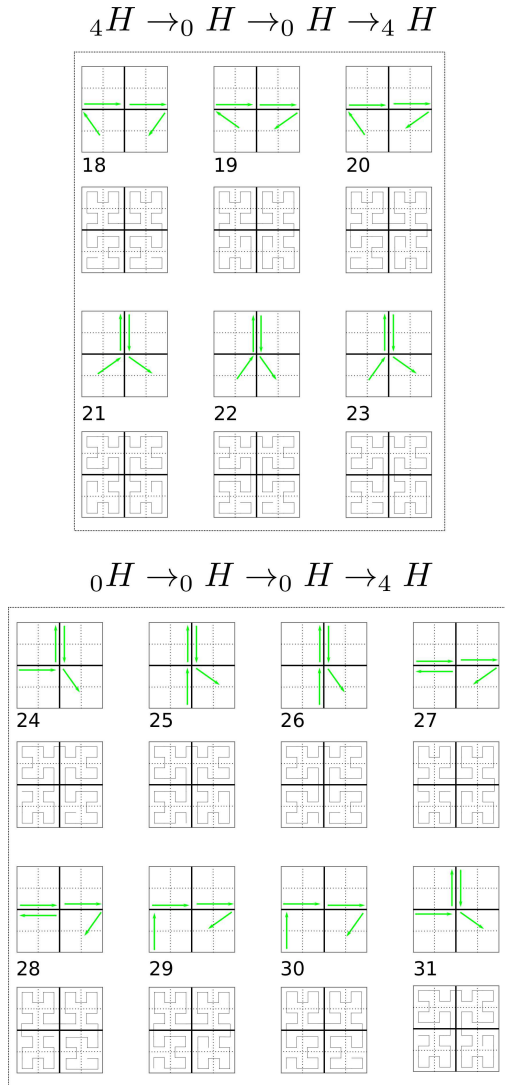


Figure 7. Inhomogeneous Hilbert curve made of a combination of ${}_0H$ and ${}_4H$ curves. Boundary vector diagrams and order 3 approximations.

3. ${}_4H + {}_0H$: The possible combinations of two boundary vectors of each type in this case will be: (a) ${}_4H \rightarrow {}_0H \rightarrow {}_0H \rightarrow {}_4H$. Another possibility is a ${}_0H$ in the first three quadrants and ${}_4H$ in the last quadrant: (b) ${}_0H \rightarrow {}_0H \rightarrow {}_0H \rightarrow {}_4H$. For (a) rotations in the 0 and 3 quadrants or in the 1 and 2 quadrants results in six new curves; while for (b) all possible rotations in each quadrant while preserving connectivity results in 8 new

curves, making a total of 14 inhomogeneous curves shown in Figure 7.

4. ${}_4H + {}_5H$: The boundary vectors of the ${}_4H$ and ${}_5H$ can not connect between any quadrant (possibilities are $0 \rightarrow 1$ or $2 \rightarrow 3$) as the connecting extreme of the boundary vector for the ${}_4H$ starts or ends at a corner, while that of ${}_5H$ start and ends at the middle of edges. Consequently this two curves can not combine at any quadrant.
5. ${}_1H + {}_0H$: The boundary vectors of the ${}_1H$ and ${}_0H$ can not connect between any quadrant (possibilities are $0 \rightarrow 1$ or $2 \rightarrow 3$) as the connecting extreme of the boundary vector for the ${}_0H$ starts or ends at a corner, while that of ${}_1H$ start and ends at the middle of the same edge. Consequently this two curves can not combine at any quadrant.
6. ${}_1H + {}_5H$: The possible combinations of two boundary vectors of each type in this case will be: (a) ${}_1H \rightarrow {}_5H \rightarrow {}_5H \rightarrow {}_1H$. Another possibility is a ${}_5H$ in the first three quadrants and ${}_1H$ in the last quadrant: (b) ${}_5H \rightarrow {}_5H \rightarrow {}_5H \rightarrow {}_1H$. Taking into account rotation at quadrant 1 and 2, (a) and (b) result in a total of six new curves shown in Figure 8.

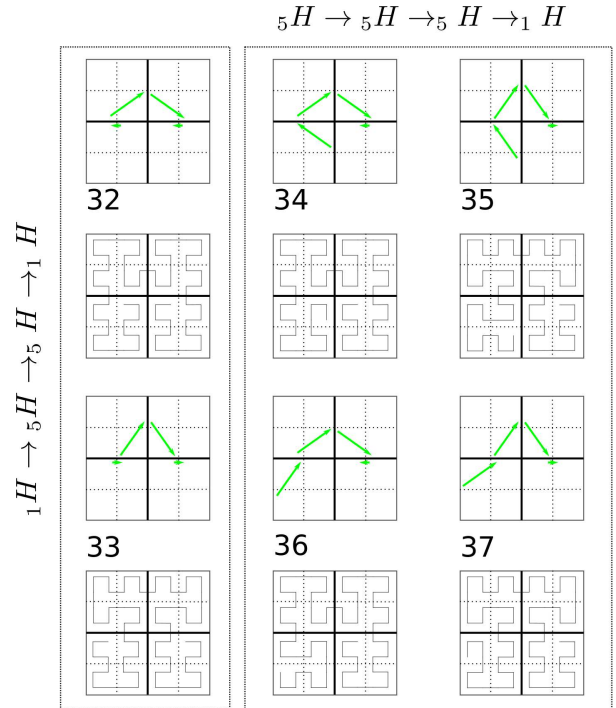


Figure 8. Inhomogeneous Hilbert curve made of a combination of ${}_5H$ and ${}_1H$ curves. Boundary vector diagrams and order 3 approximations.

7. **triplets containing ${}_0H$** : Combinations of three different curves with ${}_0H$ at quadrants 1 and 2 are not compatible with the boundary vectors, as ${}_0H$ only connects to ${}_0H$.
8. ${}_1H + {}_5H + {}_3H$: The possibility will be ${}_5H$ at quadrants 1 and 2 with ${}_1H$ and ${}_3H$, one at each remaining quadrants: (a) ${}_3H \rightarrow {}_5H \rightarrow {}_5H \rightarrow {}_1H$. Taking into account rotation at quadrants 1 and 2 results in two curves shown in Figure 9.

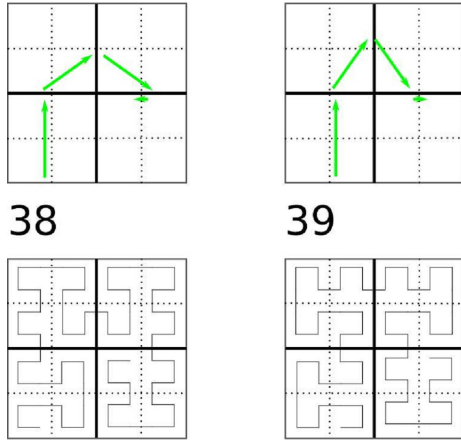


Figure 9. Inhomogeneous Hilbert curve made of a combination of $1H$, $3H$ and $5H$ curves. Boundary vector diagrams and order 3 approximations.

The sum of the inhomogeneous Hilbert curves from combinations 2), 3), 6) and 8) result in 28 possible Hilbert curves completing the proof. \square

The analytical representation of the IHHC follows the same reasoning that lead to equation (13) and will not be repeated here.

VII. BUILDING IHHC BASED ON A TAG SYSTEM

For the 28 IHHC in two dimensions the tag systems are given by:

$$\begin{aligned} 12h_{n+1} &= \delta_o(3h_n) u \overline{\delta_y(5h_n)} r 5h_n d \delta_a(3h_n) \\ 13h_{n+1} &= \delta_g(3h_n) u \delta_g(5h_n) r \overline{\delta_o(5h_n)} d \delta_x(3h_n) \end{aligned} \quad '$$

for the combination of two $3H$ and two $5H$ (Figure 6).

$$\begin{aligned} 14h_{n+1} &= \delta_o(3h_n) u \overline{\delta_y(5h_n)} r 5h_n d \delta_a(5h_n) \\ 15h_{n+1} &= \delta_g(3h_n) u \overline{\delta_g(5h_n)} r \overline{\delta_o(5h_n)} d \delta_f(5h_n) \\ 16h_{n+1} &= \delta_o(3h_n) u \overline{\delta_y(5h_n)} r 5h_n d \overline{\delta_m(5h_n)} \\ 17h_{n+1} &= \delta_g(3h_n) u \delta_g(5h_n) r \overline{\delta_o(5h_n)} d \delta_x(5h_n) \end{aligned} \quad '$$

for the combination of one $3H$ and three $5H$ (Figure 6).

$$\begin{aligned} 18h_{n+1} &= \overline{\delta_x(4h_n)} u 0h_n r 0h_n d \delta_a(4h_n) \\ 19h_{n+1} &= \overline{\delta_m(4h_n)} u 0h_n r 0h_n d \delta_f(4h_n) \\ 20h_{n+1} &= \overline{\delta_x(4h_n)} u 0h_n r 0h_n d \delta_f(4h_n) \\ 21h_{n+1} &= \overline{\delta_f(4h_n)} u \delta_g(0h_n) r \delta_x(0h_n) d \delta_m(4h_n) \\ 22h_{n+1} &= \overline{\delta_a(4h_n)} u \delta_g(0h_n) r \delta_x(0h_n) d \delta_x(4h_n) \\ 23h_{n+1} &= \overline{\delta_a(4h_n)} u \delta_g(0h_n) r \delta_x(0h_n) d \delta_m(4h_n) \end{aligned} \quad '$$

for the combination of two $0H$ and two $4H$ (Figure 7).

$$\begin{aligned} 24h_{n+1} &= \delta_m(0h_n) u \delta_g(0h_n) r \delta_x(0h_n) d \delta_x(4h_n) \\ 25h_{n+1} &= \delta_g(0h_n) u \delta_g(0h_n) r \delta_x(0h_n) d \delta_m(4h_n) \\ 26h_{n+1} &= \delta_g(0h_n) u \delta_g(0h_n) r \delta_x(0h_n) d \delta_x(4h_n) \\ 27h_{n+1} &= \delta_f(0h_n) u 0h_n r 0h_n d \delta_f(4h_n) \\ 28h_{n+1} &= \delta_f(0h_n) u 0h_n r 0h_n d \delta_a(4h_n) \\ 29h_{n+1} &= \delta_o(0h_n) u 0h_n r 0h_n d \delta_f(4h_n) \\ 30h_{n+1} &= \delta_o(0h_n) u 0h_n r 0h_n d \delta_a(4h_n) \\ 31h_{n+1} &= \delta_m(0h_n) u \delta_g(0h_n) r \delta_x(0h_n) d \delta_m(4h_n) \end{aligned} \quad '$$

for the combination of three $0H$ and one $4H$ (Figure 7).

$$\begin{aligned} 32h_{n+1} &= \delta_f(1h_n) u \overline{\delta_y(5h_n)} r 5h_n d \delta_f(1h_n) \\ 33h_{n+1} &= \delta_m(1h_n) u \delta_g(5h_n) r \overline{\delta_o(5h_n)} d \delta_m(1h_n) \end{aligned} \quad '$$

for the combination of two $1H$ and two $5H$ (Figure 8).

$$\begin{aligned} 34h_{n+1} &= \delta_f(5h_n) u \overline{\delta_y(5h_n)} r 5h_n d \delta_f(1h_n) \\ 35h_{n+1} &= \overline{\delta_a(5h_n)} u \overline{\delta_g(5h_n)} r \overline{\delta_o(5h_n)} d \delta_m(1h_n) \\ 36h_{n+1} &= \delta_x(5h_n) u \overline{\delta_y(5h_n)} r 5h_n d \delta_f(1h_n) \\ 37h_{n+1} &= \delta_m(5h_n) u \delta_g(5h_n) r \overline{\delta_o(5h_n)} d \delta_m(1h_n) \end{aligned} \quad '$$

for the combination of one $1H$ and three $5H$ (Figure 8).

Finally,

$$\begin{aligned} 38h_{n+1} &= \delta_o(3h_n) u \overline{\delta_y(5h_n)} r 5h_n d \delta_f(1h_n) \\ 39h_{n+1} &= \delta_g(3h_n) u \delta_g(5h_n) r \overline{\delta_o(5h_n)} d \delta_m(1h_n) \end{aligned} \quad '$$

for the combination of one $1H$, one $3H$ and two $5H$ (Figure 9).

VIII. CONCLUDING REMARKS

Hilbert curves have found applications in a diverse number of subjects. Literature has almost exclusively dealt with Hilbert original construction, yet, some of this applications can benefit from the availability of several curves to choose from. It has been proven that in two dimensions up to forty different Hilbert curves can be constructed. The additional twenty eight curves described in this contribution are named inhomogeneous, to point out that the $n + 1$ order curve is constructed from n order Hilbert curves of different types.

To set a sound base for the use of Hilbert curves, they need to be well understood geometrically and analytically. It is also important to know the relation between the different Hilbert curves. We have reported close analytical expressions for all HHC and IHHC, which allow to implement all mappings effectively. Also, a simple and intuitive construction procedure for all curves, based on tag system, has been reported, which gives an alternative procedure for building any of the Hilbert curve to a given finite order.

Open questions still remain, for example, numerical calculation up to high orders seems to suggest that all HHC have the same dilation factor in the infinite iterative limit, which for the original Hilbert curve was proven to be 6 [15], yet a proof of such conjecture still has not been reported. The tools developed here, could be useful in such a proof.

Computer code, developed by the authors, with the implementation of the tag system allowing the construction of all two dimensional Hilbert curves of any order can be requested (estevez@imre.uh.cu).

ACKNOWLEDGMENTS

This work was partially financed by FAPEMIG under the project BPV-00047-13. EER which to thank PVE/CAPES for financial support under the grant 1149-14-8. Infrastructure support was given under project FAPEMIG APQ-02256-12.

REFERENCES

- [1] H.-L. Chen and Y.-I. Chang, *Inf. Syst.* 30, 205 (2005).
- [2] H.-L. Chen and Y.-I. Chang, *Expert Syst. with Appl.* 38, 7462 (2011).
- [3] B. Moon, H. V. Jagadish and C. Faloutsos, *IEEE Trans. Knowl. Data Eng.* 13, 124 (2001).
- [4] Z. Songa and N. Roussopoulosb, *Inform. Syst.* 27, 523 (2002).
- [5] J.-Y. Liang, C.-S. Chen, C.-H. Huang and L. Liu, *Comp. Med. Img. and Graph.* 32, 174 (2008).
- [6] J. Zhang and S.-I. Kamata, *J. Vis. Commun. Image. R.* 23, 418 (2012).
- [7] D. A. Keim, *J. of Comp. and Graph. Stat.* 5, 58 (1996).
- [8] S. Anders, *Bioinformatics* 25, 1231 (2009).
- [9] E. Estevez-Rams, C. Perez-Davidenko, B. A. Fernandez and R. Lora-Serrano, *Comp. Phy. Comm.* 15, 118 (2015).
- [10] T. Bially, *IEEE Trans. Inf. Th.* IT-15, 658 (1969).
- [11] J. Gao and J. M. Steele, *J. Complex.* 10, 230 (1994).
- [12] J. J. Bartholdi and L. K. Platzman, *Oper. Res. Lett.* 1, 121 (1982).
- [13] D. Hilbert, *Mathematische Ann.* 38, 459 (1891).
- [14] H. Sagan, *Space-filling curves* (Springer Verlag, New York, 1994).
- [15] K. E. Bauman, *Math Notes* 80, 609 (2006).
- [16] K.-L. Chung, Y.-H. Tsai and F.-C. Hu", *IEEE Trans. Image Processing* 9, 2109 (2000).
- [17] K. Vinoy, K. Jose, V. Varadan and V. Varadan, *Microwave Symposium Digest, 2001 IEEE MTT-S International*, volume 1, 381–384 vol.1 (2001), ISSN 0149-645X.
- [18] J. Romeu and S. Blanch, *Antennas and Propagation Society International Symposium*, 2002. IEEE, volume 4, 550–553 vol.4 (2002).
- [19] J. J. Cox, Y. Takezaki, H. R. P. Ferguson, K. E. Kohkonen and E. L. Mulkay, *Computer-Aided Design* 26, 215 (1994).
- [20] E. "Skubalska-Rafajlowicz, *IEEE Trans. Inf. Th.* 47, 1915 (2001).
- [21] J. McVay, A. Hoorfar and N. Engheta, *Radio and Wireless Symposium*, 2006 IEEE, 199–202 (2006).
- [22] A. R. Butz, *IEEE Trans. Comput.* 20, 424 (1971).
- [23] S.-I. Kamata, R. O. Eason and Y. Bandou, *IEEE TransImg. Proc.* 8, 964 (1999).
- [24] E. H. Moore, *Trans. Am. Math. Soc.* 1, 72 (1900).
- [25] L. X, *Appl. Math. Comp.* 147, 741 (2004).
- [26] C. Perez-Demidenko, I. Brito-Reyez, B. Aragon-Fernandez and E. Estevez-Rams, *Appl Math and Comp* 234, 531 (2014).
- [27] P. Séébold, *Discrete Math. and Th. Comp. Sci.* 9, 213 (2007).
- [28] T. Hahn and H. Klapper, *International Table for Crystallography. Vol. A* (Kluwer Academic, 2006).